Quantummechanical oligomer approach for the calculation of vibrational spectra of polymers

C. X. Cui and Miklos Kertesz

Citation: The Journal of Chemical Physics **93**, 5257 (1990); doi: 10.1063/1.459644
View online: http://dx.doi.org/10.1063/1.459644
View Table of Contents: http://scitation.aip.org/content/aip/journal/jcp/93/7?ver=pdfcov
Published by the AIP Publishing

Quantum-mechanical oligomer approach for the calculation of vibrational spectra of polymers

C. X. Cui and Miklos Kertesz
Department of Chemistry, Georgetown University, Washington, D.C. 20057

(Received 8 February 1990; accepted 26 June 1990)

The force-constant matrix of an oligomer, composed of five or more repeat units with appropriate terminal groups, can be used to construct the force-constant matrix of the corresponding planar or helical polymer. The calculations on some typical polymers (polymeric sulfur, polyacetylene, and polyethylene) show that the oligomer approach is accurate enough to duplicate the vibrational frequencies of frozen-phonon calculations. The oligomer approach has much more predictive power if used in conjunction with some form of empirical scaling (scaled quantum-mechanical oligomer force field for polymers). ir and Raman selection rules for helical polymers are also discussed. Vibrational frequencies and intensities of polymeric sulfur and polyethylene have been calculated at the *ab initio* STO-3G, 4-31G, 6-31G, and 6-31G* basis-set levels. The agreement of frequencies with experiment is excellent. The quality of calculation is limited by the basis set and theoretical model used rather than the oligomer approach.

I. INTRODUCTION

ir and Raman techniques are very powerful in providing structural information of molecules and polymers.[1,2] The assignment of ir and Raman spectra is an essential step in elucidating their structures.[1,2] However, such assignments heavily depend on the force fields used.[1,2] Because of the large number of degrees of freedom and the difficulty in obtaining the force constants directly from experiments, sometimes it is difficult to analyze the spectra of polymers.

Although molecular-orbital methods can provide optimized geometries of molecules and polymers with a high degree of accuracy, vibrational spectra and force constants calculated by Hartree–Fock quantum chemical methods deviate systematically from the observed values.[3–6] Diagonal stretching and bending force constants are usually too high by about 10–30% for both *ab initio* and semiempirical methods. Consequently, various scaling processes for the force constants have been introduced in order to overcome this overestimation of the force constants.[4–6] A number of *ab initio* calculations show that the scaling process is successful and results in reasonable vibrational frequencies even though there are some disagreements concerning the details of the scaling process.[6d,6e]

For the vibrational analysis of polymers the empirical force-field method is widely used.[2,7] The main shortcoming of this approach is that it is difficult to find a complete set of force constants for a given polymer. Quantum chemical vibrational calculations for polymers have been carried out by the crystal-orbital method based on the frozen-phonon approach by Dewar, Yamaguchi, and Suck at the modified neglect of differential overlap (MNDO) level,[8(a)] and later by Teramae *et al.*[8(b),8(c)] and Karpfen at the *ab initio* level.[8(d)] The well-known crystal-orbital methods, which are based on the assumption that polymers have translational symmetry, suffer from the following problems.

First, the frozen-phonon approach is usually used:[9] the force constants are calculated for displacement patterns corresponding to certain vibrational normal modes (phonons), which have been determined beforehand. Generally, group theory cannot predict such displacement patterns completely. As a result, only frequencies of the vibrational modes at the $\mathbf{k} = 0$ point in the Brillouin zone, for which the atoms in each repeat unit are moving in the same way, can be obtained.[8,9] Although in principle one can enlarge the unit cell and obtain the vibrational frequencies at more $\mathbf{k}$ points, in practice this strategy is not acceptable for most systems, because the calculations become too expensive for double-, triple-, etc. sized unit cells.

Second, it is impossible to scale such a force field by the well-known methods of Pulay and co-workers[5] or other scaling schemes in order to obtain reasonable vibrational frequencies. Of course, uniform scaling[6a] is possible in connection with the frozen-phonon approach.

Third, helical polymers may have a very large translational unit cell (e.g., polymeric sulfur has 10 atoms in the translational unit cell[10]). If the helical angle is not a rational fraction of 2π, then in principle the polymer lacks translational symmetry altogether.[11] In such cases helical symmetry has to be used, which makes the calculation practicable.

In order to get insight into the problems we mentioned above, *all-trans* polyacetylene, *all-trans* polyethylene, and helical polymeric sulfur will be used as examples to show that the use of the force-constant matrix from oligomer calculations can duplicate the vibrational frequencies of polymers calculated by the crystal-orbital frozen-phonon approach. Additionally, these force constants from oligomer calculations can be used for the calculation of phonon-dispersion curves, and the scaling process of Pulay and coworkers[5] can also be applied. As a result, reasonable vibrational frequencies are obtained, and the screw axis of symmetry can be easily taken into account. We also describe

 0021-9606/90/195257-10$03.00

the selection rules for ir and Raman spectroscopy for helical polymers.

II. METHOD

A. Calculation of phonon-dispersion curves for helices

Under the assumption that a long polymer has translational symmetry, the vibrational analysis of polymers can be simplified by the use of this symmetry and Born–Kármán periodic boundary conditions.[12] More than half of the polymers whose structures have been determined by x-ray-diffraction techniques have a screw axis of symmetry.[7] In such situations the screw axis of symmetry must be used.

Here it is assumed that the harmonic approximation is applicable as it is generally accepted in the vibrational analysis of molecules and polymers.[1,2] The elements of the force-constant matrix of a polymer in terms of Cartesian coordinates can be given by

$$F_{i,j}(q_1,q_2)=\frac{\partial^2 E}{\partial X_{i,q1}\partial X_{j,q2}}, \tag{1}$$

where E is the total energy of the polymer and $X_{j,q}$ is the jth Cartesian coordinate in the qth repeat unit. For translational symmetrical systems $F_{i,j}(q_1,q_2)=F_{i,j}(q_1-q_2)$. This notation is illustrated in Fig. 1.

Indexing of the coordinates follows the Wilsonian order, i.e., for m atoms the $3m$ coordinates are arranged in the order of x,y,z for the first atom, the second atom, etc. The reciprocal-lattice vector $\mathbf{k}$ may be chosen from the $-\pi/a$ to π/a range [first Brillouin zone (BZ)] to label the vibrations of a periodic chain via the use of periodic boundary conditions.[2(a),7,12] Let $T(q)$ be the translation operator corresponding to a translation by qa, i.e., by q unit cells: $T(q)\delta X_{i,0}=\delta X_{i,q}$. ($\delta$ indicates displacement of the corresponding atomic coordinate during vibration.) The $T(q)$ operators form an Abelian group, and the symmetry-adapted displacement are[2(a),7,13]

$$\delta X_{i,q}=\exp(ikqa)\delta X_{i,0}. \tag{2}$$

Vibrational amplitudes may be normalized by making $\delta X_{i,0}$ proportional to $N^{-1/2}$, where N is the number of unit cells in the Born–Kármán period. The potential energy of the polymer in such a vibrational excited state is

$$V=\frac{1}{2}\sum_{q_1,q_2}\sum_i\sum_j F_{i,j}(q_1,q_2)\delta X^*_{i,q1}\delta X_{j,q2}. \tag{3}$$

Substitution of (2) into (3) leads to a $\mathbf{k}$-dependent potential energy expression involving only vibrational displacements in the unit cell:

$$V_k=\frac{1}{2}\sum_i\sum_j F'_{i,j}(k)\delta X_{i,0}\delta X_{j,0}, \tag{4}$$

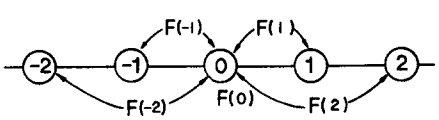

FIG. 1. Notation of the $\mathbf{F}(q)$ force-constant matrices in Eq. (1), $q=q_1-q_2$.

where (using $3m$ by $3m$ matrices)

$$\mathbf{F}'(\mathbf{k})=\mathbf{F}(0,0)+\sum_{q=\pm 1}^{\infty}\mathbf{F}(0,q)\exp(ikqa). \tag{5}$$

For localized systems, this sum converges very fast, which is behind the success of the oligomer approach. Following Wilson's GF matrix method,[1] vibrational frequencies v_i can be obtained by solving the following eigenvalue problem:

$$\mathbf{F}'(\mathbf{k})\mathbf{C}(\mathbf{k})=\mathbf{G}(\mathbf{k})\boldsymbol{\omega}(\mathbf{k})\mathbf{C}(\mathbf{k}), \tag{6}$$

where $\mathbf{G}$ is a diagonal matrix whose elements are the masses of the atoms in the repeat unit and is identical to the usual G matrix of the unit cell if Cartesian coordinates are used. The $\mathbf{C}(\mathbf{k})$ eigenvectors describe the normal modes. $\boldsymbol{\omega}(\mathbf{k})$ is a diagonal matrix whose elements, $w_j(\mathbf{k})$, are $4\pi^2 v_j(\mathbf{k})^2 c$, where $v_j(\mathbf{k})$ is the vibrational frequency of the jth phonon branch in cm^{-1} and c is the speed of light.

If a polymer has a screw axis of symmetry, the translational operators $T(q)$ will be replaced by the screw operators $S(q)$, whose action generates a rotation by an angle of $q\Theta$ around the screw axis (chosen as the $\mathbf{Z}$ axis) followed by a translation along this axis by a distance of qh. Here Θ is the helical angle and h is the translation per repeat unit as illustrated in Fig. 2 for polymeric sulfur. Wilson's GF matrix process, as described above, cannot be directly applied because the force constants (1) are expressed in Cartesian coordinates: $S(q)\delta X_{i,0}\neq\delta X_{i,q}$. However, symmetry-adapted displacements can be easily introduced:

$$\delta U_{i,q}=S(q)\delta X_{i,0}=\exp(ikqa)\delta X_{i,q}, \tag{7}$$

where $\delta U_{i,0}=\delta X_{i,0}$ and $S(q)=R(q\Theta)T(q)$, and R is a rotation operator around the Z axis. V can also be expressed in these rotated displacements:

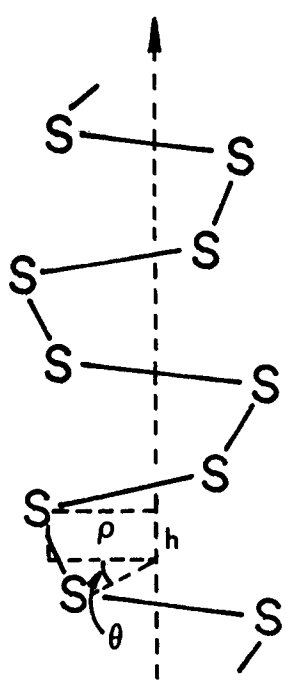

FIG. 2. Parameters to describe the helix of polymeric sulfur.

$$V=\frac{1}{2}\sum_{q_1,q_2}\sum_{i}\sum_{j}F^{\Theta}_{i,j}(q_1,q_2)\delta U^{*}_{i,q1}\delta U_{j,q2}, \qquad (3')$$

where F^{Θ} indicates that the force-constant matrix elements correspond to a rotating local coordinate system. Again, the quadratic form (3') can be reduced to a **k**-dependent one, leading to a **k**-dependent dynamical equation (6), with

$$\mathbf{F}'(\mathbf{k})=\mathbf{F}(0,0)+\sum_{q=\pm 1}^{\infty}\mathbf{F}^{\Theta}(0,q)\exp(ikqa). \qquad (5')$$

In order to make a distinction between the pure translation and the screw axis of symmetry, in the latter case it is customary to refer to the **k** values as being chosen from a pseudo-BZ, a terminology used for electronic structures of helices.[11] Computationally, it is advantageous to compute the force-constant matrix first in Cartesian coordinates, and then transform them to the symmetry-adapted form by

$$\mathbf{F}^{\Theta}(0,q)=\mathbf{F}(0,q)\mathbf{R}(q), \qquad (8)$$

where **R** is a $3m$ by $3m$ rotational matrix.

We have adopted the above method using the force constants calculated in terms of Cartesian coordinates. If the vibrational calculations were carried out in terms of the internal coordinates, transformation (8) would not be necessary, but then the process may lead to a general eigenvalue problem of a non-Hermitian complex matrix.

B. Oligomer approach for frequency calculation

The frozen-phonon approach cannot produce the complete force-constant matrix (1) because the resulting force-constant matrix is $\mathbf{F}'(\mathbf{k}=0)$ as defined in terms of $\mathbf{F}(q)$ by Eq. (5) rather than the individual $\mathbf{F}(q)$ matrices which are needed both in the scaling process and in the calculation of the complete phonon-dispersion curves, $v_j(\mathbf{k})$. The method used in this work to obtain these matrices is that the force-constant matrices $\mathbf{F}(q)$ are directly extracted from cluster or oligomer calculations. The quality of this approach improves as the size of the cluster (oligomer) increases. One can see the quality of this approximation below. For example, on the basis of this approximation, the $\mathbf{F}'(\mathbf{k})$ of polyacetylene can be approximated by identifying the force-constant matrix elements within the central repeat unit of $C_{10}H_{12}$ as $\mathbf{F}(0)$ and the force-constant matrix elements between the central and the first neighbor repeat units as $\mathbf{F}(1)$ and $\mathbf{F}(-1)$, and so on as illustrated in Fig. 3. This yields the oligomer force field for polyacetylene up to the second neighbors.

Testing of the oligomer force field has been done extensively at the NMDO level, using the computer codes developed by Stewart for molecules (MNDO-MOPAC[3(b)]) and for solids (MNDO-MOSOL[9(b)]). *Ab initio* applications are discussed in connection with scaling.

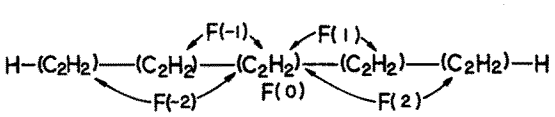

FIG. 3. $\mathbf{F}(q)$ force-constant matrices of polyacetylene from $C_{10}H_{12}$.

TABLE I. Comparison of calculated vibrational frequencies of polyacetylene (PA), polymeric sulfur (PS), and polyethylene (PE) by the MNDO frozen-phonon (MNDO-FP) approach with those by the oligomer approach in this work, including up to the second-nearest-neighbor interactions

Polymer (Θ)[a]	k($2\pi/h$)	Frequencies (cm^{-1}) MNDO-FP	MNDO-oligomer	Symmetry
PA	0.0	1267	1266	A_g
(0°)		1364	1364	A_g
		1804	1814	A_g
		3350	3352	A_g
		990	988	A_u
		1048	1046	B_g
		1296	1294	B_u
		3382	3386	B_u
PS	0.0	614	602	A_{1g}
(120°)	1/3	693	695	E_g
		242	249	E_u
PE	0.0	1191	1187	A_g
(180°)		1465	1466	A_g
		3272	3272	A_g
		1123	1123	A_u
		1181	1181	B_{3g}
		3205	3204	B_{3g}
		1336	1337	B_{3u}
	0.5	1209	1209	B_{1g}
		1488	1490	B_{1g}
		737	738	B_{1u}
		3243	3242	B_{1u}
		1234	1234	B_{2g}
		1450	1451	B_{2u}
		3295	3295	B_{2u}

[a] Θ is the helical angle.

In order to gauge the accuracy of the oligomer approximation, we have performed calculations comparing the frozen-phonon (FP) results with those of the oligomer approach including up to the second neighbors. Table I shows that the two approaches are in excellent agreement with each other. The error is usually less than 2 cm^{-1} and rarely exceeds 7 cm^{-1}. The oligomers used are shown in Fig. 4. Their geometries have been fully optimized before calculating the force constants, which is an essential step towards obtaining correct vibrational frequencies at the given level of theory.[3(a)]

The fully optimized geometrical parameters from the middle repeat unit are almost the same as those calculated by the crystal-orbital approach. The differences in bond lengths, bond angles, and dihedral angles between the two types of calculations are less than 0.002 Å, 0.5° and 0.5°, respectively.

We have chosen the oligomer $S_{11}H_2$ as a starting point for the vibrational calculations for polymeric sulfur. The calculations show that the absolute values of the matrix elements of $\mathbf{F}(q)$ are smaller than 0.001 (stretching in mdyn/Å and bending and torsion in mdyn/rad) beyond the second-nearest neighbor ($q>3$). Consequently, for localized systems such as polymeric sulfur and polyethylene the second-nearest-neighbor approximation can be considered to be converged.

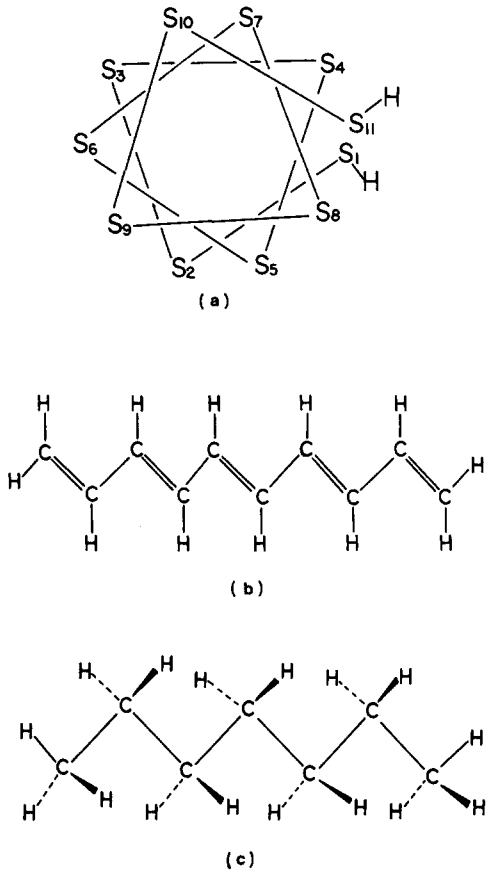

FIG. 4. The oligomers used for the extraction of force constants of (a) polymeric sulfur, (b) polyacetylene, and (c) polyethylene.

C. Oligomer approach for intensity calculation

Intensities of ir and Raman-active vibrational modes of polymers are related to dipole moment and polarizability derivatives with respect to the normal modes.[2(c)] The ir intensity for a given normal mode,

$$Q_l(\mathbf{k}) = (1/N)^{1/2} \sum_j \exp(i\mathbf{k}ja) \sum_m C^*_{l,m}(\mathbf{k}) \delta X_{m,j}, \quad (9)$$

is

$$A_l = (\pi/3c^2)|\partial\mu/\partial Q_l|^2, \quad (10)$$

where c is the speed of light and μ is the dipole moment of the polymer. The Raman-scattering activity is given by

$$I_l = 45|\alpha_l|^2 + 7\gamma_l^2, \quad (11)$$

where

$$\alpha_l = \tfrac{1}{3}(\partial\alpha_{xx}/\partial Q_l + \partial\alpha_{yy}/\partial Q_l + \partial\alpha_{zz}/\partial Q_l),$$
$$\gamma_l^2 = \tfrac{1}{2}(|\partial\alpha_{xx}/\partial Q_l - \partial\alpha_{yy}/\partial Q_l|^2 + |\partial\alpha_{zz}/\partial Q_l - \partial\alpha_{yy}/\partial Q_l|^2 + |\partial\alpha_{zz}/\partial Q_l - \partial\alpha_{xx}/\partial Q_l|^2 + 6|\partial\alpha_{xy}/\partial Q_l|^2 + 6|\partial\alpha_{yz}/\partial Q_l|^2 + 6|\partial\alpha_{xz}/\partial Q_l|^2), \quad (12)$$

where α_{ab} $(a,b = x,y,z)$ is the polarizability tensor of the polymer. For the normal mode (9) the dipole moment and polarizability derivatives can be expressed as

$$\partial\mathbf{M}/\partial Q_l(\mathbf{k}) = (1/N)^{1/2} \sum_j \exp(i\mathbf{k}ja) \times \sum_m C_{l,m}(\mathbf{k}) \partial M/\partial X_{m,j}, \quad (13)$$

where $\mathbf{M}$ might be a component of the dipole moment vector or the polarizability tensor. For translational symmetry we have

$$\partial\mathbf{M}/\partial X_{m,0} = \partial\mathbf{M}/\partial X_{m,j}, \quad j = 1,2,\ldots,N. \quad (14)$$

We can rewrite (13) as

$$\partial\mathbf{M}/\partial Q_l(\mathbf{k}) = \left[(1/N)^{1/2} \sum_j \exp(i\mathbf{k}ja)\right] \times \left[\sum_m C_{l,m}(\mathbf{k}) \partial M/\partial X_{m,0}\right] = (N)^{1/2} \delta_{\mathbf{k},0} \left[\sum_m C_{l,m}(\mathbf{k}) \partial M/\partial X_{m,0}\right]. \quad (15)$$

This formula is used in the polymer vibrational intensity calculations in such a way that the $\partial M/\partial X_{m,0}$ derivatives are calculated for the middle cell of the oligomer and combined with the $C_{l,m}$ coefficients of the $\mathbf{k}$-dependent GF analysis. From (15) the following conclusion can be obtained. The spectroscopically active modes are those at $\mathbf{k} = 0$, because dipole moment and polarizability derivatives with respect to normal mode are not zero only at $\mathbf{k} = 0$. N can be chosen as Avogadro's number. The convergence properties of Eq. (15) as a function of the size of the oligomers will be discussed in connection with the applications.

D. Force-constant scaling

Both uniform and force-constant scaling methods[4,5] of Pulay and co-workers are used for scaling the force constants of oligomers. In the uniform scaling method[6(a)] a single scaling factor is used. The scaled force-constant matrix in the method[5] of Pulay and co-workers is given by

$$\mathbf{F}_{\text{scaled}} = \mathbf{SFS}^+, \quad (16)$$

where $\mathbf{S}$ is a diagonal matrix whose elements are the square roots of the corresponding scaling factors for a given type of force constant in the internal coordinate system. Throughout this paper force-constant scaling is performed in the corresponding internal coordinate system, and then the resulting scaled force constants are transformed to those in Cartesian coordinates,[5] which in turn will be transformed according to Eq. (8) if used for a helical polymer. The scaling factors for both uniform and scaling methods of Pulay and co-workers are obtained by minimizing the error function

$$E_{\text{cr}} = \left\{\sum_i [v_i(\text{calc}) - v_i(\text{obs})]^2/(N-1)\right\}^{1/2}, \quad (17)$$

where N is the number of vibrational degrees of freedom. Tables II–IV list the experimental and calculated vibrational frequencies and intensities as well as optimized scaling factors for some small molecules.[14,15] Numbering of the atoms of n-butane is shown in Fig. 5. From this point on the scaling factors are kept constant and are used to scale the force constants of the large oligomers which in turn are used for the

TABLE II. Comparison of vibrational spectra (cm^{-1}) using scaled and unscaled 6-31G* force constants and experimental values for S_4H_2.

	6-31G*			Intensities[d]			
Expt.[a]	Scaled[b]	Scaled[c]	Unscaled	Raman	ir	Description	SF[e]
77	73	64	73	5 (5)	1 (1)	SSSS torsion	1.0145
184 S	185	171	197	7 (7)	4 (4)	SSS bend	0.8826
225 W	227	212	243	3 (3)	7 (8)		
320 VW	317	301	346	18 (19)	5 (5)	SSSH torsion	0.8423
320	322	305	350	7 (9)	41 (41)		
454 W	454	453	520	39 (38)	0 (0)	SS stretch	0.7576
484 S	484	484	556	27 (26)	7 (7)		
487	487	487	559	27 (27)	2 (2)		
851 W	853	874	1003	8 (9)	5 (5)	SSH bend	0.7234
863 W	861	882	1012	33 (33)	12 (12)		
2532 M	2536	2532	2906	60 (60)	17 (17)	SH stretch	0.7619
2540	2536	2532	2906	309 (309)	1 (1)		
E_{cr}[f]	3	14	167				

[a] After Ref. 18. Only Raman intensities were given and are indicated by S (strong), W (weak), M (medium), and VW (very weak), respectively.
[b] Scaling method of Pulay and co-workers.
[c] Uniform scaling by a factor of 0.8713.
[d] Raman and ir intensities in $Å^4$/amu and km/mol, respectively. The numbers in parentheses are scaled intensities corresponding to those by the method of Pulay and co-workers.
[e] Scaling factors for the method of Pulay and co-workers.
[f] Error function (17).

calculation of phonon-dispersion curves of the corresponding polymers.

Tables II and III show that the scaling factors for the method of Pulay and co-workers are very different when going from one type of internal coordinate to another. The results of the uniform scaling process are acceptable even though the error is 2–5 times larger than that by the method of Pulay and co-workers. The advantage of the uniform scaling is that ir and Raman intensities will not be affected upon scaling. The intensities for the scaled and unscaled force fields are given in Tables II and IV and the intensities of the unscaled force fields are equal to those by the uniform scaling. Note that the intensities for the scaled force field obtained by the method of Pulay and co-workers do not lead to significant improvement in comparison with the unscaled results for the above two molecules. Therefore, only intensities for the unscaled force field are given for polymers.

TABLE III. Optimized force-constant scaling factors or butane.

	Scaling factors	
Description	4-31G	STO-3G
C_2–C_3 stretch	0.9041[a]	0.7436
C_1–C_2 stretch	0.8805	0.6872
CCC bend	0.8502[a]	0.8835
CCCC torsion	0.7848[a]	0.6883
C_1–H_5 stretch	0.8377	0.6289
C_2–C_1–H_5 bend	0.7485	0.6269
C_3–C_2–C_1–H_5 torsion	0.7775	0.6147
C_1–H_7 stretch	0.8419	0.6313
C_2–C_1–H_7 bend	0.7719	0.6404
C_3–C_2–C_1–H_7 torsion	0.7602	0.6334
C_2–H_{11} stretch	0.8101[a]	0.6242
C_3–C_2–H_{11} bend	0.7732[a]	0.6812
C_4–C_3–C_2–H_{11} torsion	0.7752[a]	0.6216

[a] Scaling factors and interval coordinates used for the force-constants scaling of polyethylene (see Table VIII).

E. Selection rules

Vibrational selection rules for the normal modes of polymers have been given by Higgs and Tobin.[16] The only spectroscopically active modes are those with $\mathbf{k} = 0$, i.e., totally symmetrical under the translational group. One can simply illustrate this selection rule: Let us consider such a vibrational mode, which can produce a dipole moment in the unit cell along the z axis. At $\mathbf{k} = 0$, the dipoles generated by the vibrations of the atoms in the unit cells point in the same direction as shown in Fig. 6(a). The total dipole moment of the polymer is not zero and the mode is ir active. At $\mathbf{k} = \pi/a$,

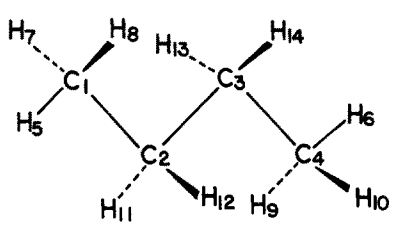

FIG. 5. Numbering of the atoms of *n*-butane.

TABLE IV. A comparison of observed and calculated vibrational frequencies (cm^{-1}) of *n*-butane by scaled force constants.

	4-31G			Intensities[d]	
Expt.[a]	Scaled[b]	Scaled[c]	Unscaled	Raman	ir
A_u 102	111	113	126	0	0
A_u 194	206	212	235	0	0
B_g 225	236	243	270	0	0
B_u 271	264	259	287	0	0 (0)
A_g 425	428	418	463	4 (3)	0
A_u 731 S	714	732	811	0	4 (4)
A_g 803	798	815	907	0 (0)	0
B_g 837	828	819	903	16 (17)	0
A_u 948 M	944	958	1074	0	1 (1)
B_u 964 M	960	969	1062	0	3 (9)
B_u 1009 W	1006	1003	1112	0	6 (0)
A_g 1059	1066	1025	1136	18 (19)	0
A_g 1151	1155	1164	1290	6 (6)	0
B_g 1180	1184	1216	1348	2 (2)	0
A_u 1257 W	1258	1289	1429	0	0 (0)
B_g 1300	1290	1324	1467	29 (29)	0
B_u 1290 W	1306	1338	1483	0	1 (1)
A_g 1361	1358	1387	1537	2 (1)	0
B_u 1379 M	1383	1427	1582	0	8 (4)
A_g 1382	1384	1428	1582	5 (9)	0
A_g 1442	1446	1493	1655	47 (63)	0
B_u 1460 S	1451	1495	1656	0	3 (5)
B_g 1460	1458	1500	1662	44 (44)	0
A_u 1461 S	1461	1501	1663	0	15 (15)
A_g 1461	1461	1503	1666	22 (15)	0
B_u 1461 S	1472	1511	1675	0	8 (7)
A_g 2853	2848	2853	3162	70 (149)	0
B_u 2853	2854	2860	3170	0	64 (81)
A_g 2872	2864	2865	3178	319 (149)	0
B_u 2870 S	2890	2867	3175	0	82 (60)
B_g 2912	2912	2870	3181	190 (244)	0
A_u 2930 S	2911	2891	3204	0	15 (74)
B_g 2965	2970	2921	3238	78 (104)	0
A_g 2965	2970	2925	3242	174 (171)	0
B_u 2968 S	2971	2926	3244	0	116 (107)
A_u 2968 S	2972	2928	3246	0	172 (127)
E_{cr}[f]	9	32	198		

[a] Expt. ir intensities are indicated by S (strong), M (medium), and W (weak), respectively (Ref. 14).
[b] Scaled force field by the method of Pulay and co-workers.
[c] Uniform scaling by a factor of 0.9022.
[d] Raman and ir intensities in $Å^4$/amu and km/mol, respectively. The intensities based on the scaled force field by the method of Pulay and co-workers are given in parentheses.
[f] Error function (17).

those dipoles are arranged in such a way that the two nearest dipoles point in the opposite direction as presented in Fig. 6(b). In this situation the total dipole moment is zero. As a result, this mode will not be ir active. For the intermediate value of **k** the dipole moments average to zero over a range of the size $2\pi/\mathbf{k}$. The same idea can be used to understand the polarizability change of a vibrating polymer which gives rise to Raman scattering.[1,2] The symmetry analysis of spectroscopically active modes of polymers can be carried out by the use of the factor group.[2,16] For helical polymers, the situation is more complicated, especially for a helical polymer with a helical angle which is an irrational fraction of 2π, and no factor group exists.

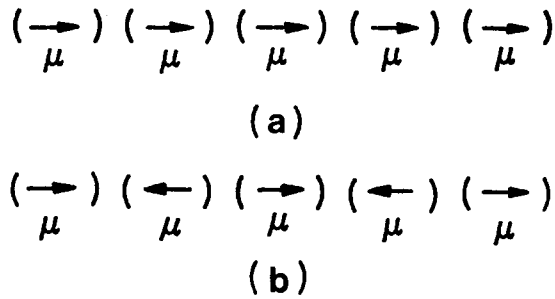

FIG. 6. The direction of dipole moments from each repeat unit at (a) $\mathbf{k} = 0$ and (b) π/a.

Let us identify those displacement vectors, which transform as x,y,z, or xy, yz, zx, $x_2 - y^2$, $x^2 + y^2$, and z^2 by first using the omnipotent time-reversal symmetry[13] for the phonon branches

$$v_j(-\mathbf{k}) = v_j(\mathbf{k}). \tag{18}$$

For any given **k** this allows us to combine pairs of complex symmetry-adapted displacements for a helix (7) into real ones

$$\delta U'_{i,q} = \cos(kqa)\delta U_{i,0}, \tag{19}$$

$$\delta U''_{i,q} = \sin(kqa)\delta U_{i,0}. \tag{20}$$

For specific values of **k** these displacements will be ir or Raman active with the corresponding polarizations, by matching the helical angle:

$\mathbf{k} = 0$: Eqs. (11) and (12) are totally symmetrical and transform like z or $x^2 + y^2$ and z^2 with respect to the screw operation, $S(q)$ (ir and Raman active).

$\mathbf{k} = \Theta/a$: Eqs. (11) and (12) transform as x and y or xz and yz with respect to $S(q)$ (ir and Raman active).

$\mathbf{k} = 2\Theta/a$: Eqs. (11) and (12) transform as xy and $x^2 - y^2$ with respect to $S(q)$ (Raman active only).

These selection rules are extensions of those given by Zerbi[2(d)] for helical angles, which are rational fractions of 2π.

III. APPLICATION OF THE OLIGOMER APPROACH TO POLYMERIC SULFUR AND *ALL-TRANS* POLYETHYLENE

A. Polymeric sulfur

The optimized geometries of polymeric sulfur by the crystal-orbital method at the MIDI-1* basis set and semiempirical levels have been reported earlier.[17,11] The optimized geometrical parameters from the middle section of the S_5H_2 oligomer at the STO-3G, 6-31G, and 6-31G* levels and the helical angle (which is a derived parameter) are listed in Table V together with the available experimental and theoretical data. One can see that the oligomer approach has the same power as the crystal-orbital method to predict the geometry of polymeric sulfur.

According to the selection rules outlined above, there should be six Raman-active and two ir-active modes for a monatomic helix. The corresponding frequencies for polymeric sulfur at the STO-3G, 6-31G, and 6-31G* levels are listed in Table VI together with intensities at the 6-31G*

TABLE V. Optimized geometrical parameters of polymeric sulfur based on the middle section of the small oligomer S_5H_2 using various basis sets and compared with available crystal-orbital calculations and experiments.

Method	S–S (Å)	SSS (deg)	SSSS (deg)	Θ (deg)
STO-3G	2.072	103.6	84.0	108.4
4-31G	2.233	103.4	78.9	105.4
6-31G	2.210	105.4	79.7	104.8
6-31G*	2.061	106.9	80.1	104.1
MIDI-1* [a]	2.084	105.1	79.7	104.9
DF[b]	2.233	109.0	86.5	107.0
	2.312	83.5	91.0	124.0
Expt.[c]	2.07	106.0	86.5	108.0

[a] Crystal-orbital result [Ref. 17(a)].
[b] Density-functional crystal orbital results and two minima found [Ref. 17(b)].
[c] Reference 18(c).

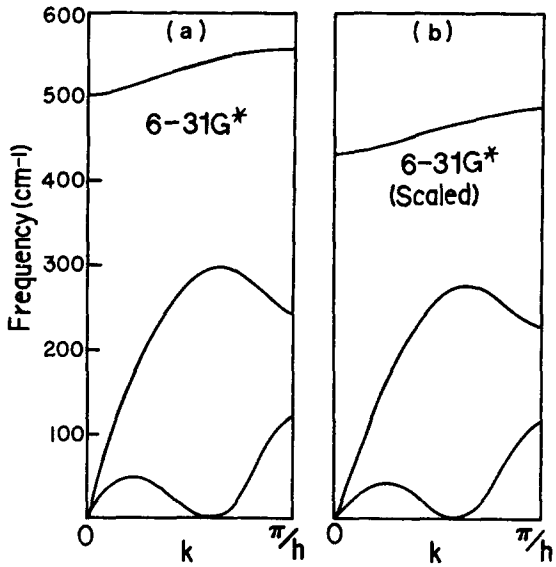

FIG. 7. Calculated (a) unscaled and (b) scaled phonon-dispersion curves of polymeric sulfur based on the oligomer S_5H_2 at the 6-31G* level. Best uniformly scaled dispersion curves can be obtained from (a) by multiplying it by a factor of 0.8713.

level, based on the S_5H_2 oligomer. The three internal coordinates and the corresponding scaling factors are taken from Table II. The phonon-dispersion curves calculated by the use of the unscaled and scaled force constants of S_5H_2 at the 6-31G* level are shown in Fig. 7.

The frequencies corresponding to the translational and rotational motions of the polymer as a whole, which should be zero, are extremely sensitive to the accuracy of the calculated force constants as well as the accuracy of the solution of the eigenvalue problem, particularly for the rotational motion. The squares of the frequencies corresponding to the translational and rotational modes of somewhat large molecules are usually found to be between $\pm$ 900 cm^{-2}.[3(a)] Similar errors have been found in our calculations by the frozen-phonon approach.[9(b)] However, the modes with vibrational frequencies larger than 50 cm^{-1} are not affected significantly. Due to these errors in the 0–50 cm^{-1} energy range we have interpolated the phonon-dispersion curves in this range by using only the calculated frequencies above 50 cm^{-1} and the $v(\mathbf{k}) = 0$ modes which are determined by symmetry. Actually, the calculated lowest frequencies are not completely out of line. For example, at the 6-31G* level at $\mathbf{k} = 0$ and $\mathbf{k} = \Theta$ the lowest calculated frequencies are 4.3 and 1.8 cm^{-1}, respectively, instead of being zero.

No Raman spectrum has been reported for perfect helical polymeric sulfur,[18] because of the difficulty to obtain single crystals. As compared with the available data on amorphous samples, the basic features of the calculated spectrum are reasonable at all levels reported in Table VI. It has been shown by Pulay *et al.*[5] that the *ab initio* force field at the split basis-set level is essential to obtain a reasonable scaled force field for a variety of molecules. For sulfur, *d* functions play an important role in S–S bonding. As a result, we believe that the results at the scaled 6-31G* level are most reliable in Table VI. The frequencies of S–S stretching are between 410 and 490 cm^{-1}, corresponding to the highest phonon-dispersion curve in Fig. 7. The S–S–S bending modes between 300 and 100 cm^{-1} can be associated with the middle dispersion curve, while the S–S–S–S torsion corre-

TABLE VI. Calculated vibrational spectra of polymeric sulfur.

	Calc. (cm^{-1})					Intensities[d]		
k[a]	STO-3G	6-31G	6-31G*	6-31G* [b]	6-31G* [c]	Raman	ir	Description
0	620	422	502	436	437	16	0	S-S stretch
$\pm \Theta/h$	308	239	292	278	255	14	1	SSS bend
	675	458	538	471	469	6	1	S–S stretch
$\pm 2\Theta/h$	34	55	55	52	48	13	0	SSSS torsion
	277	239	266	267	255	16	0	SSS bend
	686	478	549	480	478	3	0	S–S stretch

[a] Θ corresponds to the helical angle of polymeric sulfur in Table V.
[b] SQMOFF, scaling factors taken from Table II (S_4H_2).
[c] Uniform scaling by the scaling factor from Table II.
[d] ir and Raman intensities in km/mol and $Å^4$/amu, respectively.

TABLE VII. Optimized and observed geometrical parameters of all-*trans* polyethylene and its oligomers.

Method	r(C–C) (Å)	r(C–H) (Å)	∠CCC (deg)	∠HCH (deg)
C_5H_{12} (STO-3G)[a]	1.545	1.089	112.5	107.1
C_7H_{16} (STO-3G)[a]	1.545	1.088	112.4	107.1
C_5H_{12} (4-31G)[a]	1.532	1.087	113.2	106.5
C_5H_{12} (6-31G)[a]	1.533	1.088	113.3	106.3
C_5H_{12} (6-31G*)[a]	1.530	1.089	113.4	106.2
STO-3G CO[b]	1.547	1.089	112.6	107.0
Expt.	1.53	1.07	112	107

[a] From the middle repeat unit of the oligomer.
[b] Crystal-orbital approach by Karpfen and Beyer (Ref. 19). Somewhat different results were reported by Teramae *et al.* [Refs. 8(c) and 20] based on less-converged calculations.

sponds to frequencies below 120 cm^{-1}. The lowest two phonon-dispersion curves correspond to acoustic vibrational modes, the slope of which at $\mathbf{k} = 0$ is related to sound velocity and Young's modulus of the polymer.

Because this polymer can freely translate along the **X**, **Y**, and **Z** axes and rotate around the **Z** axis, there should be four zero frequencies which correspond to those translational and rotational motions. Since the translation along the **Z** axis and rotation around **Z** axis belong to the $\mathbf{k} = 0$ irreducible representation, two of the zero frequencies should be at $\mathbf{k} = 0$. The translations along the **X** and **Y** axes belong to the irreducible representation of $\mathbf{k} = \Theta/h$. Therefore, the two frequencies at $\mathbf{k} = \pm \Theta/h$ should be zero, as illustrated in Fig. 7.

B. Polyethylene

All-trans polyethylene has a twofold screw axis of symmetry. The optimized geometry of *all-trans* polyethylene has been reported at various basis-set levels.[19,8(b)] The corresponding geometrical parameters are compared with those obtained from oligomer calculations and experimental data in Table VII. Similar to the situation of polymeric sulfur the oligomer approach gives almost the same results as that of the *ab initio* crystal-orbital calculation if comparable basis sets are used. The same strategy as that of polymeric sulfur is used to obtain the vibrational frequencies from the scaled force constants of C_5H_{12}. The reason that we use the smaller oligomer C_5H_{12}, rather than C_7H_{14}, is that the difference between the two phonon-dispersion curves is less than 5 cm^{-1} at the STO-3G level. Therefore, we do not expect that the results will be significantly different upon increasing the size of the oligomer. The resulting spectroscopically active frequencies at the STO-3G, 4-31G, and 6-31G* levels as well as the frequencies at the scaled 4-31G level, together with experimental data, are listed in Table VIII. The internal coordinates and corresponding scaling factors are indicated in Table III. The resulting frequencies by the scaled quantum-mechanical oligomer force-field (SQMOFF) approach are in excellent agreement with the experimental data.[14]

The phonon-dispersion curves obtained at the 6-31G*, 4-31G, and scaled 4-31G levels are presented in Fig. 8. The scaled phonon-dispersion curves are almost the same as those obtained by the empirical force field which are determined by fitting experimental frequencies.[21]

The symmetry labels and descriptions of the vibrational modes of polyethylene are presented in Table VIII. The

TABLE VIII. Comparison of experimental and calculated vibrational frequencies (cm^{-1}) of *all-trans* polyethylene by the oligomer approach.

		Calc. (cm^{-1})					
k	Expt.[a]	STO-3G	4-31G	6-31G*	4-31G[b]	4-31G[c]	Description
0	A_u 1050	1278	1190	1162	1046	1074	CH_2 twist
	A_g 1131	1336	1220	1223	1138	1101	CC stretch
	B_{3g} 1168	1439	1344	1316	1184	1213	CH_2 rock
	B_{3u} 1176	1439	1356	1319	1195	1223	CH_2 wag
	A_g 1440	1825	1653	1638	1454	1491	CH_2 scissor
	A_g 2848	3600	3159	3182	2844	2850	CH_2 *s*-stretch
	B_{3g} 2883	3708	3228	3189	2852	2912	CH_2 *a*-stretch
π/h	B_{1u} 725	834	797	780	702	719	CH_2 rock
	B_{1g} 1061	1264	1140	1139	1075	1029	CC stretch
	B_{2g} 1295	1569	1459	1451	1284	1316	CH_2 twist
	B_{1g} 1370	1765	1536	1574	1362	1386	CH_2 wag
	B_{2u} 1468	1855	1679	1664	1478	1515	CH_2 scissor
	B_{2u} 2851	3607	3171	3190	2854	2861	CH_2 *s*-stretch
	B_{1u} 2919	3732	3228	3243	2905	2912	CH_2 *a*-stretch
E_{er}[d]			207		16	33	

[a] After Ref. 14.
[b] SMQOFF, scaling factors based on butane (Table III).
[c] Uniform scaling by the scaling factor (0.9022) from Table IV.
[d] Error function (17).

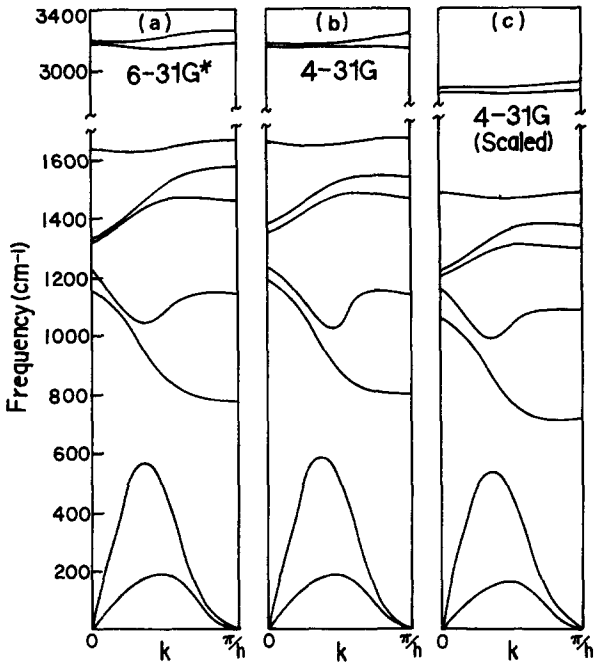

FIG. 8. Calculated phonon-dispersion curves of polyethylene at the (a) 6-31G*, (b) 4-31G, and (c) 4-31G scaled level based on the oligomer C_5H_{12}. Best uniformly scaled dispersion curves can be obtained from (b) by multiplying it by a factor of 0.9022.

highest two dispersion curves in Fig. 8(c) and 2850 cm^{-1} correspond to the C–H stretching vibrations. The third from about 1450 cm^{-1} describes the CH_2 scissor vibrations. Due to the small interaction between the local C–H stretching and CH_2 scissor vibrations the above three dispersion curves are very flat. The fourth, fifth, and seventh curves describe the CH_2 twisting and rocking. The sixth dispersion curve corresponds to C–C stretching. The lowest two are acoustic modes like that of polymeric sulfur in Fig. 7. The slope of the longitudinal acoustic branch (second lowest) at $\mathbf{k} = 0$ is much larger than that of the corresponding acoustic branch for polymeric sulfur, which in that case is the slope of the lowest branch corresponding to torsional dispersion. Therefore, Young's modulus of polyethylene is much higher than that of polymeric sulfur.

The calculated vibrational intensities of polyethylene at the STO-3G and 6-31G levels are listed in Table IX. The results at the STO-3G level for three different oligomers show that the convergence is faster for frequencies than for the intensities. The intensities at the 6-31G level are in much better agreement with experiment than those at the STO-3G level. In general, it seems that the quality of the intensity calculations is not limited by the oligomer approach but rather by the basis-set plus electron correlation.

IV. CONCLUSIONS

In this work a new strategy is proposed to calculate the phonon-dispersion curves of polymers based on empirical scaling of quantum-mechanically calculated oligomer force fields (SQMOFF). The use of the force-constant matrix from oligomer calculations leads to reproduction of the vibrational frequencies of the polymers at $\mathbf{k} = 0$ as obtained for the infinite periodic polymer by the frozen-phonon approach. As compared with the frozen-phonon approach, the advantages of the SQMOFF approach are as follows. (a) Complete phonon-dispersion curves can be calculated. (b) Either the scaling method of Pulay and co-workers or a uni-

TABLE IX. The calculated vibrational intensities[a] of PE.

	STO-3G (C_5H_{12})		STO-3G (C_7H_{16})		STO-3G (C_9H_{21})		6-31G (C_7H_{16})		
Symmetry	Freq.	Inten.	Freq.	Inten.	Freq.	Inten.	Freq.	Inten.	Expt.[b]
				ir-active modes					
B_{1u}	834	2.4	833	2.2	835	2.1	796	0.9	S
A_u	1277	0.0	1278	0.0	1278	0.0	1186	0.0	VVW
B_{3u}	1439	8.0	1438	8.2	1438	8.6	1356	0.4	VW
B_{2u}	1855	0.0	1854	0.0	1854	0.0	1675	1.5	S
B_{2u}	3607	9.4	3608	9.9	3607	9.1	3174	44.4	S
B_{1u}	3732	8.6	3733	8.2	3733	8.1	3233	43.5	S
				Raman-active modes					
B_{1g}	1264	9.7	1262	10.4	1263	11.1	1150	4.7	M
A_g	1336	6.7	1339	7.2	1338	7.4	1229	4.4	M
B_{3g}	1438	1.5	1437	1.5	1434	1.4	1337	0.0	W
B_{2g}	1568	23.3	1566	22.3	1567	25.1	1449	11.4	M
B_{1g}	1765	0.4	1766	0.3	1766	0.2	1539	0.0	VW
A_g	1825	22.3	1826	22.3	1826	22.3	1652	13.8	M
B_g	3600	58.7	3601	55.9	3601	54.5	3166	66.5	S
B_{3g}	3708	48.1	3709	46.2	3709	45.1	3176	50.8	S

[a] ir and Raman intensities in $Å^4$/amu and km/mol, respectively, and correspond to the unscaled or uniform scaled force field.

[b] Expt. intensities are given by S (strong), M (medium), W (weak), VW (very weak), and VVW (very very weak) after Ref. 14.

form scaling technique can be applied in order to obtain improved vibrational frequencies. (c) A screw axis of symmetry can be easily taken into account.

The application of the oligomer approach to polymeric sulfur and polyethylene shows that this approach at the scaled *ab initio* level can give results which are in excellent agreement with experimental frequencies. The intensities depend on the basis set much more than the frequencies. The oligomer approach produces intensities and frequencies for polymers at about the same quality as expected from the same basis set for a similar molecule.

Finally, we would like to point out that when using the SQMOFF approach, one should be careful about the choice of the terminal groups. Different terminal groups might give completely different results, especially if the polymer has two energetically close isomorphs.[22,23]

ACKNOWLEDGMENTS

This work has been supported by a grant from the National Science Foundation (No. DMR-8702148). We are indebted to Dr. S. Kafafi for his help with the *ab initio* calculations. We thank Dr. P. Pulay for allowing us to use his force-constant transformation program and an anonymous referee for urging us to include the calculated intensities in the paper and other comments.

[1] E. B. Wilson, Jr., J. C. Decius, and P. C. Cross, *Molecular Vibrations* (McGraw-Hill, New York, 1955).

[2] (a) J. C. Decius and R. M. Hexter, *Molecular Vibrations in Crystals* (McGraw-Hill, New York, 1977); (b) J. K. Koenig, Appl. Spectrosc. Rev. **4**, 233 (1971); (c) *Vibrational Intensities in Infrared and Raman Spectroscopy*, edited by W. B. Person and G. Zerbi (Elsevier, New York, 1982); (d) G. Zerbi, Appl. Spectrosc. Rev. **2**, 193 (1969).

[3] (a) W. J. Hehre, L. Radom, P. v. S. Schleyer, and J. A. Pople, *Ab Initio Molecular Orbital Theory*, (Wiley, New York, 1986); (b) M. J. S. Dewar and W. Thiel, J. Am. Chem. Soc. **99**, 4899 (1977); **99**, 4907 (1977).

[4] W. Meyer and P. Pulay, J. Chem. Phys. **56**, 2109 (1972); P. Pulay and F. Torok, Mol. Phys. **25**, 1153 (1973).

[5] P. Pulay, G. Fogarasi, F. Pang, and J. E. Boggs, J. Am. Chem. Soc. **101**, 2550 (1979); P. Pulay, G. Fogarasi, G. Pongor, J. E. Boggs, and A. Vargha, J. Am. Chem. Soc. **105**, 7037 (1983); G. Fogarasi and P. Pulay, Vib Spectra Struct. **14**, 125 (1985).

[6] (a) S. Saebo, L. Radom, and H. F. Schaefer III, J. Chem. Phys. **78**, 845 (1983); (b) A. Peluso, M. Seel, and J. Ladik, Can. J. Chem. **63**, 1533 (1985); (c) B. A. Hess, Jr., L. J. Schaad, P. Carsky, and R. Zahradnik, Chem. Rev. **86**, 7096 (1986), and references herein; (d) S. Dasgupta and W. A. Goddard III, J. Chem. Phys. **90**, 7207 (1989); (e) J. S. Alper, H. Dothe, and M. A. Lowe, Chem. Phys. Lett. **163**, 571 (1989); (f) P. L. Polavarpu, Chem. Phys. Lett. **163**, 576 (1989).

[7] H. Tadokoro, *Structure of Crystalline Polymers* (Wiley, New York, 1979).

[8] (a) M. J. S. Dewar, Y. Yamaguchi, and S. H. Suck, Chem. Phys. **43**, 145 (1979); (b) H. Teramae, T. Yamabe, and A. Imamura, J. Chem. Phys. **81**, 3564 (1984); (c) H. Teramae, T. Yamabe, C. Satoko, and A. Imamura, Chem. Phys. Lett. **101**, 149 (1983); (d) A. Karpfen, J. Phys. C **12**, 3227 (1979).

[9] (a) W. Weber, in *The Electronic Structure of Complex Systems*, edited by P. Phariseau and W. M. Temmerman, (Plenum, New York, 1984); (b) The MOSOL package designed for MNDO crystal-orbital calculations contains an option for frozen-phonon calculations. See J. J. P. Stewart, OCPE Bull. **5**, 61 (1985); and *MOSOL Manual* (USAF, Colorado Springs, 1984).

[10] S. Geller and M. D. Lind, Acta Crystallogr. Sec. B **25**, 2166 (1969).

[11] C. X. Cui and M. Kertesz, J. Am. Chem. Soc. **111**, 4216 (1989); C. Zheng, R. Hoffmann, and D. R. Nelson (unpublished); I. I. Ukrainskii, Theor. Chim. Acta **38**, 139 (1975).

[12] J. G. Kirkwood, J. Chem. Phys. **9**, 506 (1937); L. Piseri and G. Zerbi, J. Mol. Spectrosc. **26**, 254 (1968).

[13] M. Lax, *Symmetry Principles in Solid State and Molecular Physics* (Wiley, New York, 1974); N. W. Ashcroft and N. D. Mermin, *Solid State Physics* (Sounders, Philadelphia, 1976).

[14] T. Shimanouchi, *Tables of Molecular Vibrational Frequencies*, Natl. Stand. Ref. Data Ser. Natl. Bur. Stand. (U.S. GPO, Washington, DC, 1972).

[15] F. Feher, W. Laue, and G. Winkhaus, Z. Anorg. Allg. Chem. **288**, 113 (1956); H. Wieser, P. J. Krueger, E. Muller, and J. B. Hyne, Can. J. Chem. **47**, 1633 (1969).

[16] P. W. Higgs, Proc. R. Soc. London, Ser. A **220**, 472 (1953); M. C. Tobin, J. Chem. Phys. **23**, 891 (1955); C. Y., Liang, J. Mol. Spectrosc. **1**, 61 (1957).

[17] (a) A. Karpfen, Chem. Phys. Lett. **136**, 571 (1987); (b) M. Springborg and R. O. Jones, Phys. Rev. Lett. **57**, 1145 (1986).

[18] (a) T. Ward, J. Phys. Chem. **72**, 4133 (1986); (b) H. L. Strauss and J. A. Greenhouse, in *Elemental Sulfur: Chemistry and Physics* (Interscience, New York, 1965); (c) F. Tuinstra, Acta Crystallogr. **20**, 341 (1966).

[19] A. Karpfen and A. Beyer, J. Comput. Chem. **5**, 11 (1984).

[20] H. Teramae, J. Chem. Phys. **85**, 990 (1986); H. Teramae (private communication, 1989).

[21] T. Tasumi, T. Shimanouchi, and T. Miyazawa, J. Mol. Spectrosc. **9**, 261 (1962); **11**, 422 (1963).

[22] C. X. Cui, M. Kertesz, and Y. Jiang, J. Phys. Chem. **94**, 5172 (1990).

[23] J. Kürti and P. R. Surjan, J. Chem. Phys. **92**, 3247 (1990).